

© 2014 IEEE. Personal use of this material is permitted. Permission from IEEE must be obtained for all other uses, in any current or future media, including reprinting/republishing this material for advertising or promotional purposes, creating new collective works, for resale or redistribution to servers or lists, or reuse of any copyrighted component of this work in other works.

Digital Object Identifier (DOI): <http://dx.doi.org/10.1016/j.microrel.2014.07.069>

Microelectronics Reliability, vol. 54, no. 9, pp. 1935-1939, 2014

Impact of active thermal management on power electronics design

Markus Andresen

Marco Liserre

Suggested Citation

Andresen, Markus, and Marco Liserre. "Impact of active thermal management on power electronics design." Microelectronics Reliability 54.9 (2014): 1935-1939.

Impact of active thermal management on power electronics design

M. Andresen^{a,*}, M. Liserre^a

^a Chair of Power Electronics, Christian-Albrechts-University of Kiel, Kaiserstraße 2, 24143 Kiel, Germany

Abstract

Power electronic system design is typically constrained by the thermal limitation so by the overall losses and the peak current. To stay within the maximum current, reached only during transients, the system is typically overrated. Active thermal management is used to control the maximum temperature and the temperature swing to reduce failures that are mostly caused by them. In this paper it is proposed to use the active thermal management to reduce the switching losses or to move them to less stressed devices, during transients, such as a module can reach an higher current, without violating thermal constraints, and the need of overdesign can be reduced. Hence an optimal and cost effective design of power electronics system is achieved.

Corresponding author.

ma@tf.uni-kiel.de

Tel: +49 (431) 880 6107; Fax: +49 (431) 880 6103

Impact of active thermal management on power electronics design

M. Andresen^{a,*}, M. Liserre^a

1. Introduction

PWM voltage source converters have become widely used in several applications like traction, automotive or the generation of renewable energies [1], [2]. The design of the system has to be cost effective, guaranteeing reliability at the same time. However, overdesign is a common practice to reduce failures, especially during transients, avoiding too high temperatures or excessive thermal swings.

This work proposes the use of a thermal management system not only for reducing failures related to overtemperature or temperature swings [3], but also for achieving a loss reduction in transient conditions to enable a better utilization of the existing hardware.

First, this work analytically analyzes thermal cycling of the junction temperature in an inverter and highlights how different operating conditions constrain the junction temperature. Practical examples how the thermal management system can control the losses with a benchmark of the possible stress reduction are given in chapter 4. Conclusions for system design with thermal management are given in chapter 5 and the results are summarized in chapter 6.

2. Thermal models of power electronic modules

During operation, the power semiconductors cause losses P_{loss} , which are mainly generated by switching losses P_{sw} and conduction losses P_{cond} .

$$P_{loss} = P_{sw} + P_{cond} \quad (1)$$

The losses cause heating of the devices, which affects the operation of the semiconductors. Thereby excessive temperatures, which are approximately 150° C for silicon, lead to an increased failure rate. In general high temperatures in the range (20° C - 150° C) increase the losses and reduce the lifetime, while thermal cycling affects aging of the semiconductors,

also being the prevalent reason for failures [4]. The chip size and the power semiconductor heat transfer capability influence the heat dissipation, whereby a decrease of the chip area worsens the heat transfer capability. This can be expressed in an increase of the thermal resistance R_{th} . The thermal resistances define the correlation of a temperature difference and the corresponding losses P_{loss} between two points (e.g. junction to case $R_{th,jc}$). For stationary analysis, the averaged junction temperature $T_{j,av}$ can be expressed with

$$T_{j,av} = T_c + R_{th,jc} \cdot P_{loss} \quad (2)$$

For a more accurate calculation for the transient temperature T_{inv} in an inverter at the time t_{end} , the calculation has to be made for every single switching operation.

$$T_{inv}(t_{end}) = \sum_{k=1}^{k_{end}} (P_{loss,k} - P_{loss,k-1}) \cdot \sum_{i=1}^n R_{th,i} (1 - \exp(-\frac{t_{end} - t_{k-1}}{\tau_i})) \quad (3)$$

In this equation, the losses in each switching position are expressed with $P_{loss,k}$ and the switching frequency with f_s [5]. The parameter $R_{th,i}$ and τ_i are the datasheet values of the Foster thermal network. Using these datasheet values does not necessarily lead to the precise junction temperature, because of parameter variations that result from the production process and aging effects [6]. However, these values obtain a safety margin to prevent overheating introduced by the manufacturer.

The times t_k represent switching times and can generally be expressed with (4) and (5), whereas $\Theta(k)$ depends on the modulation scheme and k_{end} represents the sample of the last switch before t_{end} .

* Markus Andresen. ma@tf.uni-kiel.de
Tel: +49 (431) 880 6107; Fax: +49 (431) 880 6103

$$t_{2k-1} = \left(\frac{1 - \Theta(k)}{2} + k - 1 \right) T_s \quad (4)$$

$$t_{2k} = \left(\frac{1 + \Theta(k)}{2} + k - 1 \right) T_s \quad (5)$$

For optimized utilization of three phase voltage source inverter, the maximum linearity is exploited by using SVPWM (space vector modulation) with added 1/6 of the 3rd harmonic:

$$\Theta(k) = m \cdot \left(\cos(2\pi k \frac{f_0}{f_s} + \varphi) + \frac{1}{6} \cos(6\pi k \frac{f_0}{f_s} + 3\varphi) \right) \quad (6)$$

The losses of the power semiconductors have to be calculated for each switching state. For an IGBT, the switching losses $P_{sw,T}$ and the conduction losses $P_{cond,T}$ can be expressed with:

$$P_{sw,T}(k) = f_s (E_{on} + E_{off}) \cdot \frac{\hat{i} \cdot \cos(2\pi \cdot k \cdot \frac{f_0}{f_s} + \varphi)}{I_{ref}} \cdot \left(\frac{V_{out}}{V_{ref}} \right)^c \quad (7)$$

$$P_{cond,T}(k) = \left(\hat{i} \cdot \sin(2\pi \cdot k \cdot \frac{f_0}{f_s} + \varphi) \right) \cdot u_{ce,sat} + r_{ce} \cdot \hat{i}^2 \cdot \sin^2(2\pi \cdot k \cdot \frac{f_0}{f_s} + \varphi) \cdot \frac{t_k}{T_s} \quad (8)$$

In these equations, \hat{i} is the magnitude of the current, E_{on} and E_{off} are the turn on/off losses at reference current and voltage, φ is the phase displacement of the current to the voltage, V_{out} is the voltage blocked by the semiconductor, V_{ref} and I_{ref} are the reference values for the measurement of the semiconductor losses and c is an empirical factor estimated to $c = 1.35$ [5]. The conduction losses of the IGBT are linearized with the constant voltage drop $u_{ce,sat}$ and the current magnitude dependent voltage

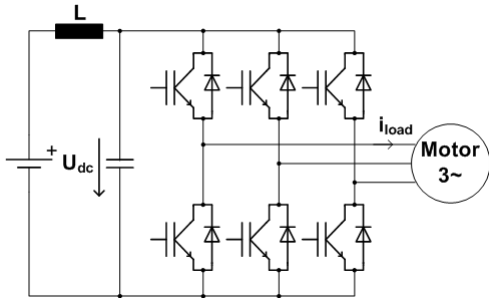


Fig. 1: Simplified drivetrain of an electrical vehicle

drop r_{ce} . It needs to be mentioned, that the losses are only affected during the turn on time for positive voltage and positive current at the semiconductors. Similar to the IGBT, the losses for the diodes $P_{sw,D}$ and $P_{cond,D}$ can be expressed.

$$P_{sw,D}(k) = f_{sw} \cdot E_{rr} \cdot \left(\frac{\hat{i} \cdot \cos(2\pi \cdot k \cdot \frac{f_0}{f_s} + \varphi)}{I_{ref}} \right)^d \cdot \left(\frac{V_{out}}{V_{ref}} \right)^d \quad (9)$$

$$P_{cond,D}(k) = \left(\hat{i} \cdot \sin(2\pi \cdot k \cdot \frac{f_0}{f_s} + \varphi) \right) \cdot u_D + r_D \cdot \hat{i}^2 \cdot \sin^2(2\pi \cdot k \cdot \frac{f_0}{f_s} + \varphi) \cdot \frac{t_{on,k}}{T_s} \quad (10)$$

The parameter d is an empirical factor for the losses and is set to $d = 0.6$, while u_D and r_D represent the linearization of the diode forward characteristics. Losses are only generated for positive voltages and negative currents.

For demonstration an electrical vehicle with a 2-level voltage source inverter fed by a battery system is chosen such as in Fig. 1. By applying (4) with a DC-link voltage $U_{dc} = 700$ V, the modulation scheme of (6), a phase displacement $\varphi = 0$ and a modulation factor $m = 1.16$, the maximum conduction time for the IGBT is chosen. The case temperature is set to $T_c = 80$ °C and an output current $\hat{i} = 25$ A is fed, which is similar to the rated DC current of the selected power module [7]. The fundamental frequency is $f_0 = 50$ Hz and the switching frequency is $f_s = 2.5$ kHz. Furthermore, the temperature calculated by using the average losses $T_{j,av}$, calculated with (2), is shown in the

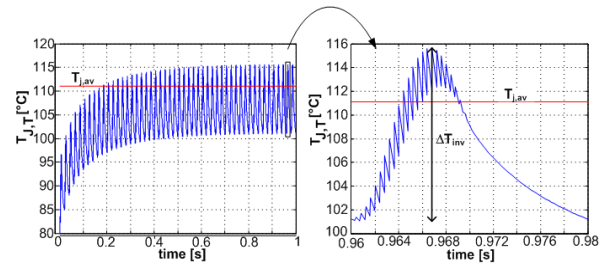


Fig. 2: Junction temperature of an IGBT in a PWM inverter ($\hat{i} = 25$ A, $U_{dc} = 700$ V, $f_{sw} = 2.5$ kHz): exact calculation (blue) averaged loss calculation (red)

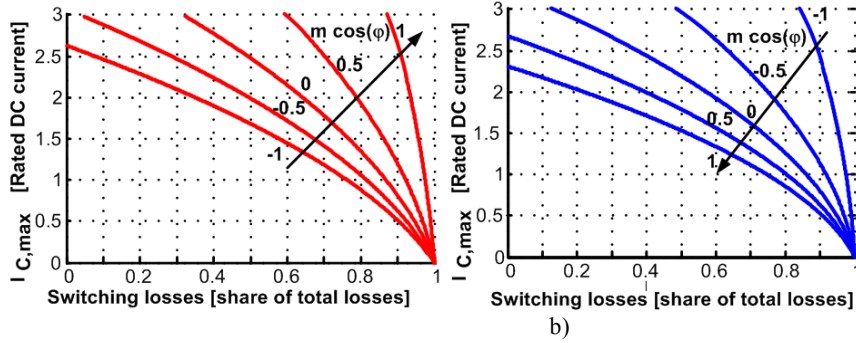


Fig. 4: Analytic maximum semiconductor current for constant total losses in a voltage source inverter: a) Diode b) IGBT

figure. It can be observed, that the thermal cycles obtain a magnitude of $\Delta T_{inv} = 15.5 K$. The temperature, which has been calculated by using the averaged losses, is within the thermal cycling of the precise calculation, but exceeds the average temperature.

3. Active thermal management

Since thermal cycling and high temperatures cause the aging of power electronic modules, the thermal swing has to be kept as small as possible. An approach to prevent excessive thermal cycling is to control the junction temperature in critical conditions [3]. A severe condition for inverters is to feed a variable speed drive, such as an electrical vehicle, with high torque and low speed. This effect is known for accelerated failures in power converters used for doubly-fed induction generators in wind applications [8]. Because of the low fundamental frequency, the time for heating up and cooling down are very high and thus the thermal cycles are high. This occurs for example during acceleration of a vehicle. For a better understanding, the effect of constant power and varying fundamental frequencies on the maximum temperature $T_{inv,max}$ is analyzed in Fig. 3 for the conditions similar to Fig. 2.

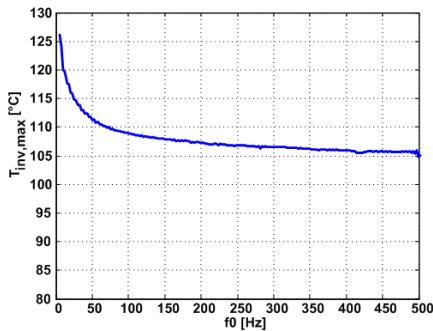


Fig. 3: Junction temperature in dependence of output frequency for constant current magnitude

It can be seen that the maximum junction temperature is very high for low output frequencies. At the same time, the magnitude of the thermal cycles increases, because the time for cooling down is longer. For frequencies above 200 Hz, this effect gets less crucial. To overcome the problem of accelerated aging caused by low output frequencies, a limitation of the output current in dependence of the output frequencies is recommended, even if this affects the performance of the application.

Another possibility, to reduce stress in operation, is a variable switching frequency. A minimum switching frequency, which is set in transient conditions, would reduce the stress for the inverter, enabling a maximum collector current, which is higher than the nominal DC collector current, limited only by the semiconductor manufacturers to $2 \cdot I_{c,dc,max}$ or $3 \cdot I_{c,dc,max}$ [5]. In Fig. 4, the influence of the switching frequency on the maximum collector current $I_{c,max}$ is visualized. For this figure, the overall losses are constant on the curves. These constant losses divide in the conduction losses, approximated with (8) and (10), and the switching losses, which are expressed as the share of the overall losses. Different curves represent different values of $m \cdot \cos(\varphi)$ for a module with the datasheet values of [7]. It can be seen, that the stress is distributed between the devices and either the diodes or the IGBTs are limiting the output current.

The switching frequency has also an impact on the thermal cycles ΔT_{inv} , which is presented in Fig. 4 for different output currents. The range of the switching frequency is typical for automotive applications. As expected, the thermal swing increases with higher output current and higher switching frequency. However, reduced switching losses cause higher current harmonics and thus higher losses in a possible

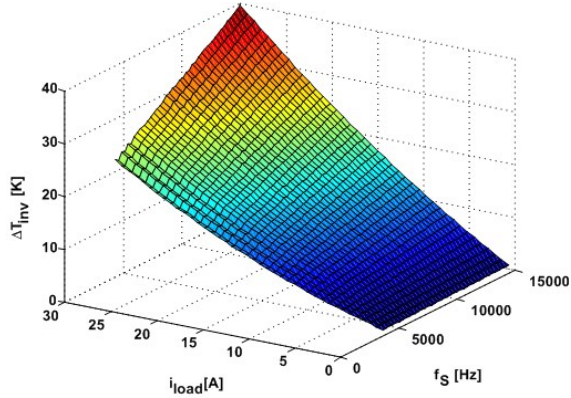


Fig. 5: Thermal cycles of the junction temperature in dependence of load current and switching frequency

connected motor, which is why low switching frequencies are not desired in steady state operation. Nevertheless, for transient conditions it is feasible to keep losses and thus the thermal swing in the inverter constant. As it can be seen in Fig. 5, a reduction of the switching frequency by 50% enables an approximately 25% higher current under a constant thermal swing. Another interesting approach is to change the loss distribution in the inverter. The losses of a half bridge usually distribute between the IGBTs and the diodes. Thereby in application under full load with $\cos(\varphi) > 0$, the current is mainly conducted in the IGBTs, while for $\cos(\varphi) < 0$, the current is mainly conducted in the freewheeling diodes. Hence the loss distribution is dependent on the phase displacement between voltage and current, as shown in Fig. 6. For some applications it might be interesting to accept higher total losses, but control has been applied for a maximum torque per ampere strategy in [2]. reduced losses for a single semiconductor. A possible way to realize this is to change the dc link voltage. For the control of a drive it is also possible to set a thermal optimum for the inverter, distributing the losses between the semiconductors with a higher magnetization, instead of a maximum torque per ampere. In traction applications

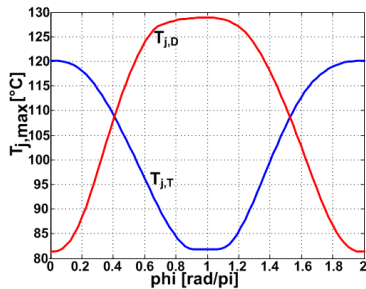


Fig. 6: Maximum junction temperature for IGBT and diode for constant apparent power and $T_c = 80^\circ C$

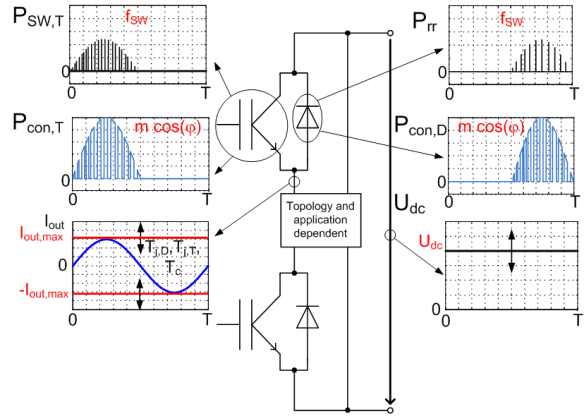


Fig. 7: Variables in the proposed thermal management system (red) for an inverter

a dc link voltage

4. Impact of active thermal management on inverter operation

The potential for the introduced thermal management strategies depend highly on the system and its mission profile, which is addressed in [9]. Possible control variables of the thermal management system are shown in Fig. 7. Changeable parameters are the switching frequency, the modulation index m and a maximum temperature limitation for the protection of the devices. For the modulation index, there is either the possibility to implement discontinuous modulation to reduce the switching frequency and the current conduction paths [10] or to adjust the dc link voltage. In the following, two different mission profiles are taken and the stress reduction is evaluated with (3). Transients caused by the current controller are neglected.

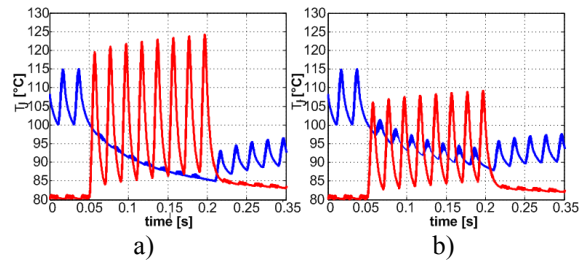


Fig. 8: Junction temperature (IGBT blue, Diode red) for change between consumption and generation ($i_{load}=25 A, f_s = 8 \text{ kHz}$): a) without thermal management system b) with thermal management system increasing the dc-link voltage by 100%

4.1. Reverse power variation

Firstly the case of an electrical vehicle is shown in Fig. 8. At the beginning, the inverter is feeding power to the motor and after 50 ms, the vehicle is braking and the inverter is operating in rectifying mode until $t=0.2s$, when reduced power is again fed into the motor. In case of no thermal management system, the diodes of the inverter are highly stressed during the rectifying operation and the junction temperature rises up to $T_{j,D} = 125^{\circ}C$. To reduce this stress, the dc-link voltage is increased from $U_{dc} = 500V$ to $U_{dc} = 1000V$, what reduces the magnitude of the current and also changes the modulation index. The doubling of the voltage is used only for demonstrating the differences, while the real boost factor depends on the module choice. As it can be seen in Fig. 8 b), the maximum temperature is reduced to $110^{\circ}C$ and the thermal swing is reduced to 30 K, compared to 45 K without the management system.

4.2. Curve climbing

The second case shows worst case conditions by means of a fixed rotor with high torque. Because of the fixed rotor, a DC current is fed into the machine, affecting maximum stress to single semiconductors while others are not conducting the current. In worst case, the full magnitude is conducted in one semiconductor while the high switching frequency also causes high switching losses. This case is visualized in Fig. 9 for the half rated DC current with and without a thermal management system. Without the management system the temperature increases up to $T_{j,max} = 140^{\circ}C$ for the IGBT, while the thermal management system facilitates to reduce the switching losses, leading to a IGBT junction temperature of only $T_{j,max} = 119^{\circ}C$. Thus the stress is efficiently reduced. Disadvantageous for this strategy is a reduced dynamic of the controller caused by the higher sampling periods. However, the strategy to reduce the switching frequency can also be

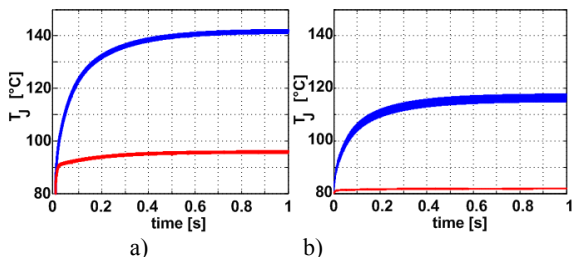


Fig. 9: Junction temperature (IGBT blue, Diode red) for curve climbing ($i_{load}=12.5A$, $U_{dc}=500V$): a) Without thermal management system for $f_s = 8kHz$ b) With thermal management system reducing $f_s = 8kHz$ to $f_s = 1kHz$

used to reduce the thermal swing caused by a short period of increased active power.

5. Impact of active thermal management in system design

As shown, an active thermal management system enables to reduce stress during transient conditions, leading to a better utilization and reduced stress for semiconductors. For the utilization of this potential, the mission profile of an inverter needs to be analyzed in Fig. 10. The mission profile leads to the voltage range V_{ces} , which determines the length of the space charge region and the maximum apparent power S_{max} , which determines the preliminary maximum current rating. The modulation index m and the ratio between active and apparent power $\cos(\varphi)$, also part of the mission profile, indicate, which components are most stressed and they contribute in defining the voltage and current limitations hence to choose the right power electronics topology. In parallel, the thermal conditions are considered: the cooling system is chosen considering the ambient temperature $T_{ambient}$ and the losses, consequence of the electrical design, such as the maximum junction temperature $T_{j,max}$ and the maximum magnitude of the thermal cycles ΔT_{max} . The preliminary ratings are checked for expected transient conditions, in which the thermal management system can reduce the stress. Taking into account the approximated stress reduction of 10% for specific conditions, the rating of the modules can be reduced by the same rate for applications which undergo the described profiles.

6. Conclusion

A thermal management system enables loss redistribution and reduction. That can increase the overloading capability of power electronic modules, especially during transients, and facilitates good chip utilization without affecting the functionality. Using

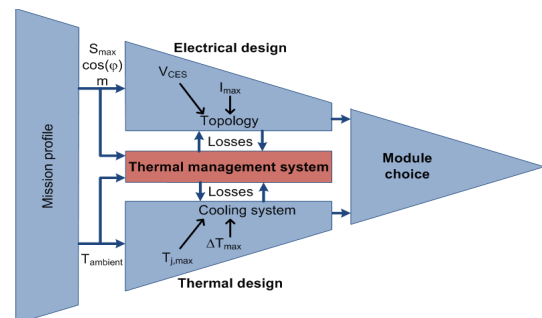


Fig. 10: Process of choosing a power electronic module

active thermal management in the system design process can reduce the rating of the power semiconductors.

7. Acknowledgement

This study was funded under the ERC Consolidator Grant 2014-2019 in the project “Highly Efficient and Reliable smart Transformer” (HEART).

References

- [1] R. Teodorescu, M.Liserre, P. Rodriguez. Grid converters for photovoltaic and wind power systems. John Wiley & Sons. (2011)
- [2] J. Lemmens, P. Vanassche, J. Driesen. Optimal Control of Traction Motor Drives under Electro-Thermal Constraints. IEEE Journal of Emerging and Selected Topics in Power Electronics, R-2 (2014) pp. 249-263.
- [3] D.A. Murdock, J.E.R. Torres, R.D. Lorenz. Active thermal control of power electronic modules. IEEE Trans. Industry Applications. R-42 (2006) pp. 552-558.
- [4] Huai Wang, M. Liserre, F. Blaabjerg, P. de Place Rimmen, J.B. Jacobsen, T. Kvisgaard, J. Landkildehus. Transitioning to Physics-of-Failure as a Reliability Driver in Power Electronics. IEEE Journal of Emerging and Selected Topics in Power Electronics. R-2 (2014) pp. 97-114
- [5] A. Wintrich, U. Nicolai, W. Tursky, T. Reimann. Application Manual Power Semiconductors. ISLE, 2011
- [6] A. Pigazo, M. Liserre, F. Blaabjerg, T. Kerekes. Robustness analysis of the efficiency in PV inverters. Convergence of the IEEE Industrial Electronics Society (2013) pp 7015-7020.
- [7] Infineon, Datasheet of FS25R12W1T4_B11
- [8] M. Bartram, J. Bloh, R.W. De Doncker. „Doubly-fed-machines in wind-turbine systems: is this application limiting the lifetime of IBTS-frequency-converters?. IEEE Power Electronics Specialits Conference. (2004) pp. 2583-2587
- [9] M. Andresen, M. Liserre. Review of Active Thermal Control and Lifetime control Techniques for power electronic modules. Conference on Power Electronics and Applications (EPE). (2014) pp. N.N. accepted for publication
- [10] M. Weckert, J. Roth-Stielow. Chances and limits of a thermal control for a three-phase voltage source inverter in traction applications using permanent magnet synchronous or induction machines. IEEE Conference on Power Electronics and Applications (EPE). (2011) pp. 1-10.